Interaction and Adhesion Properties of Polyelectrolyte Multilayers

ARTICLE *in* LANGMUIR · SEPTEMBER 2005

Impact Factor: 4.46 · DOI: 10.1021/la051045m · Source: PubMed

4 AUTHORS, INCLUDING:

Krasimir Vasilev
University of South Australia
84 PUBLICATIONS **1,653** CITATIONS
SEE PROFILE

Olga I Vinogradova
Russian Academy of Sciences
111 PUBLICATIONS **3,385** CITATIONS
SEE PROFILE

Interaction and Adhesion Properties of Polyelectrolyte Multilayers

Haofei Gong,[†] Javier Garcia-Turiel,[†,‡] Krasimir Vasilev,[†] and Olga I. Vinogradova*[,†,§]

Max Planck Institute for Polymer Research, Ackermannweg 10, 55128 Mainz, Germany, van't Hoff Institute for Molecular Sciences, University of Amsterdam, Nieuwe Achtergracht 166, 1018 WV Amsterdam, The Netherlands, and Laboratory of Physical Chemistry of Modified Surfaces, A.N.Frumkin Institute of Physical Chemistry and Electrochemistry, Russian Academy of Sciences, 31 Leninsky Prospect, 119991 Moscow, Russia

Received April 19, 2005. In Final Form: June 8, 2005

The growth, morphology, and interaction/adhesion properties of supported poly(sodium 4-styrenesulfonate)/poly(allylamine hydrochloride) (PSS/PAH) and DNA/PAH multilayers were investigated by means of surface plasmon resonance spectroscopy, atomic force microscope (AFM) imaging, and AFM-related force measurements. Multilayers were assembled on a prelayer of poly(ethylenimine) (PEI) both with and without drying. SPR results showed a linear growth of the assembly in the case of PSS/PAH multilayers and nonlinear growth for DNA/PAH multilayers. Measurements of forces acting between a bare glass sphere and a multilayer-coated surface indicated repulsive or attractive forces, depending on surface charge, which suggests that, on approach, electrostatic forces dominate. On separation, we observed large pull-off forces in the case of positively charged multilayers and weak pull-off forces in the case negatively charged multilayers. Multiple adhesions and plateau regions observed on separation were interpreted in terms of a bridging of multiple polymer chains between the glass particle and the multilayer and a stretching of the polyelectrolyte loops. The dependence of the pull-off force on the number of deposited layers shows regular oscillations.

1. Introduction

The alternate deposition of polycations and polyanions on a charged surface leads to the buildup of films known as polyelectrolyte multilayers.[1−4] These films have attracted considerable attention during the past decade due to their potential applications in various fields, ranging from nanomechanical composites and electrochemical devices to biomaterial and optical coatings.[5] This, in turn, has opened a whole new area of surface engineering dealing with the coated colloids, polyelectrolyte microcapsules,[6−10] and nanotubes.[5,11,12]

Despite numerous publications on the assembly and characterization of polyelectrolyte multilayers, information about interaction and adhesion properties of multilayer-coated surfaces is rather scarce. To our knowledge, there have been only a few publications on the subject.[13−17] Nearly all of them studied the interaction between poly(styrenesulfonate)/poly(allylamine hydrochloride) (PSS/PAH) multilayers.[18−20] These multilayers are known to growth linearly with the number of deposition steps,[21] and their structure is often assumed to be stratified.[22] Direct force measurements have been first performed[13] with the interferometric surface force apparatus (SFA) technique.[23] Although these experiments have shed some light on some questions surrounding the interaction behavior of PSS/PAH multilayer coated surfaces, there have been some limitations. In contrast to the commonly used conditions of multilayer assembly,[3] the multilayers reported in ref 13 were prepared from diluted polyelectrolyte solutions with low ionic strength. This research was recently extended into studying PSS/PAH multilayers deposited under more commonly used conditions.[14] Both interferometric SFA and noninterferometric surface force apparatus (MASIF)[23] have been used. The number of adsorbed monolayers was limited to two[13] or four,[14] so that this should be considered as a precursor, but not true, multilayer regime, and the results of both publications might strongly be influenced by the substrate (mica and/or glass). Indeed, an atomic force microscope (AFM)

* Corresponding author. E-mail: vinograd@mpip-mainz.mpg.de.
† Max Planck Institute for Polymer Research.
‡ University of Amsterdam.
§ Russian Academy of Sciences.

(1) Decher, G. *Science* **1997**, *277*, 1232−1237.
(2) Knoll, W. *Curr. Opin. Colloid Interface Sci.* **1996**, *1*, 137−143.
(3) Bertrand, P.; Jonas, A.; Laschewsky, A.; Legras, R. *Macromol. Rapid Commun.* **2000**, *21*, 319−348.
(4) Schonhoff, M. *J. Phys.: Cond. Matter* **2003**, *15*, R1781−R1808.
(5) Hammond, P. T. *Adv. Mater.* **2004**, *16*, 1271−1293.
(6) Caruso, F.; Caruso, R. A.; Mohwald, H. *Science* **1998**, *282*, 1111−1114.
(7) Donath, E.; Sukhorukov, G. B.; Caruso, F.; Davis, S.; Möhwald, H. *Angew. Chem.* **1998**, *37*, 2202−2205.
(8) Sukhorukov, G. B.; Donath, E.; Lichtenfeld, H.; Knippel, E.; Budde, A.; Mohwald, H. *Colloids Surf. A* **1998**, *137*, 253−266.
(9) Vinogradova, O. I. *J. Phys.: Condens. Matter* **2004**, *16*, R1105−R1134.
(10) Caruso, F. *Adv. Mater.* **2001**, *13*, 11.
(11) Lang, Z. J.; Susha, A. S.; Yu, A. M.; Caruso, F. *Adv. Mater.* **2003**, *15*, 1849−1853.
(12) Mayya, K. S.; Gittins, D. I.; Dibaj, A. M.; Caruso, F. *Nano Lett.* **2001**, *1*, 727−730.
(13) Lowack, K.; Helm, C. A. *Macromolecules* **1998**, *31*, 823−833.
(14) Blomberg, E.; Poptoshev, E.; Claesson, P. M.; Caruso, F. *Langmuir* **2004**, *20*, 5432−5438.
(15) Bosio, V.; Dubreuil, F.; Bogdanovic, G.; Fery, A. *Colloids Surf. A* **2004**, *243*, 147−155.
(16) Kulcsar, A.; Voegel, J. C.; Schaaf, P.; Kekicheff, P. *Langmuir* **2005**, *21*, 1166−1170.
(17) Kulcsar, A.; Lavalle, P.; Voegel, J. C.; Schaaf, P.; Kekicheff, P. *Langmuir* **2004**, *20*, 282−286.
(18) Ramsden, J. J.; Lvov, Y. M.; Decher, G. *Thin Solid Films* **1995**, *254*, 246−251.
(19) Caruso, F.; Niikura, K.; Furlong, D. N.; Okahata, Y. *Langmuir* **1997**, *13*, 3422−3426.
(20) Picart, C.; Ladam, G.; Senger, B.; Voegel, J. C.; Schaaf, P.; Cuisinier, F. J. G.; Gergely, C. *J. Chem. Phys.* **2001**, *115*, 1086−1094.
(21) Ruths, J.; Essler, F.; Decher, G.; Riegler, H. *Langmuir* **2000**, *16*, 8871.
(22) Garza, J. M.; Schaaf, P.; Muller, S.; Ball, V.; Stoltz, J. F.; Voegel, J. C.; Lavalle, P. *Langmuir* **2004**, *20*, 7298−7302.
(23) Parker, J. L. *Prog. Surf. Sci.* **1994**, *47*, 205.

10.1021/la051045m CCC: $30.25
Published on Web 07/09/2005

study[15] suggested that the true PSS/PAH multilayer regime, where the influence of substrates disappears, corresponds to at least six deposited layers. This is in agreement with a recent interferometric SFA study[16] of the interaction and adhesion properties of PSS/PAH multilayers performed with films consisting of eight or nine polyelectrolyte monolayers, which led to results different than early publications.[13,14] Beside these researches focused on PSS/PAH films, the interaction between exponentially growing poly(L-glutamic acid) (PGA)/poly(L-lysine) (PLL) multilayers performed with the interferometric SFA technique has been reported.[17]

In this paper, we study the interaction between a bare glass sphere with a supported (glass) multilayer film. This experimental configuration is different from all previous studies, where both surfaces were coated by polyelectrolyte films.[13−17] Both commonly used PSS/PAH multilayers and similarly prepared DNA/PAH multilayers were explored with surface plasmon resonance spectroscopy (SPR), atomic force microscope (AFM) imaging, and force measurements. The multilayers were assembled on a prelayer of poly(ethylenimine) (PEI). Since all previous publications on the subject have dealt with flexible polyelectrolytes, our work represents the first attempt to study and to compare the interaction/adhesion properties of multilayers based both on highly flexible (PSS/PAH) and a semiflexible polyelectrolyte (DNA/PAH). We found that a clear nonlinearity of the film growth for DNA/PAH multilayers and their special internal structure with long-range ordering also made them very different from linearly[14−16] and exponentially[17] growing films. In our work, we measure the interaction and adhesion properties for systems consisting to up to five bilayers of polyelectrolytes, which allows us to explore both "precursor" and "true" multilayer regimes. Beside that, we address the influence of drying on the properties of the multilayers: the films we study here are assembled both with and without drying.

2. Experimental Section

2.1. Materials. The polyelectrolytes used for the preparation of the self-assembled films were poly(ethylenimine) (PEI, 50% w/v, $M_w \sim 1200$ g/mol) and poly(allylamine hydrochloride) (PAH, $M_w \sim 70\,000$ g/mol) as polycations and poly(sodium 4-styrenesulfonate) (PSS, $M_w \sim 70\,000$ g/mol) and deoxyribonucleic acid (DNA double helix, $M_w \sim 6\,000\,000$ g/mol, sodium salt, from calf thymus) as polyanions. All were purchased from Sigma-Aldrich Chemie GmbH and were used as received. No additional buffers were added to the polyelectrolyte solutions to adjust the pH value. NaCl was purchased from Aldrich (purity > 99%). Index oil was obtained from Winopal Forschungsbedarf GmbH. 3-Mercaptopropionic acid (3MPA) was purchased from Aldrich. Water used in experiments was obtained by using a commercial Milli-Q system containing ion-exchange and charcoal stages and had a resistivity higher than 18 MΩ/cm.

The microscope glass slides used as supporting substrates (76 × 26 mm^2) were purchased from Menzel-Glaser. Borosilicate glass microspheres of radius 10 ± 1.0 μm were purchased from Duke Scientific Corp. Tipless V-shaped cantilever were obtained from NanoProbes. The glass prism and LaSFN9 substrates for surface plasmon experiments were purchased from Hellma Optik.

2.2. Procedure. Glass slides were cleaned following a two step procedure. The first step included cleaning by means of piranha solutions, i.e., submerging the slides under a 3:1 (vol %) mixture of sulfuric acid and 30% hydrogen peroxide for at least 20 min at 80 °C. This allows removal of organic residues from the substrates. The second step was performed according to the RCA protocol.[24] This included immersion in 5:1:1 (vol %) H_2O/H_2O_2/NH_3 mixed solution at 80 °C for ca. 15 min, followed by extensive rinsing with Milli-Q water. After such a cleaning procedure, slides were completely hydrophilic. In all experiments, a prelayer of PEI was adsorbed on the glass substrate by immersion (30 min) into a 1.0 mg/mL aqueous solution of PEI. After adsorption, the films were rinsed by continuously dipping them three times for 5 min each in Milli-Q water.

Multilayer films were then formed on the PEI-coated glass substrates by sequential deposition of polyanions and polycations. All polyelectrolyte solutions, except DNA, were of a concentration of 1 mg/mL and contained 0.5 M NaCl. The adsorption of DNA was performed from 0.5 mg/mL solutions that also contained 0.5 M NaCl.[25] The samples were manually dipped into the polyelectrolyte solutions for 20 min (PSS/PAH film) and 40 min (DNA/PAH film) each. After rinsing with water three times for 5 min each, the multilayer was dried in air or dipped into the oppositely charged polyelectrolyte solution immediately without drying.[26]

2.3. Characterizations. *2.3.1. Surface Plasmon Resonance Spectroscopy (SPR).* A home-built surface plasmon resonance spectrometer (SPR) was used for measurements of the multilayer film thickness. The sample was attached to the base of a glass prism optically matched by index oil in a Kretschmann configuration. The beam of a HeNe laser ($\lambda = 632.8$ nm, JDS Uniphase Corp.) with transverse-magnetic polarization was directed through the prism. By rotating the prism, the angle of the incident beam relative to the surface was adjusted. Collection of the reflected light with a photodiode mounted on a second collinear goniometer allows for angle-resolved reflectivity measurements. For more details, see refs 27 and 28.

To prepare substrates for SPR measurements, a gold layer with a thickness of 50 nm was thermally evaporated on high refractive index ($n = 1.8$) LaSFN9 slides. The gold film was then functionalized by a self-assembled monolayer of 3MPA, as the substrates were immersed in a 0.03 mol/L solution of 3MPA for 24 h. Such a modified surface was negatively charged in water due to the dissociation of carboxylic groups belonging to the 3MPA. The multilayer buildup was conducted in a Teflon flow cell attached to the sample surface, allowing measurements in solution. Briefly, the solution of polyelectrolyte was injected into the flow cell and the required time was allowed for deposition. Then the sample was washed with a sufficient volume of Milli-Q water and a SPR scan was performed. At least three measurements at different positions on the surface of the sample were done after the deposition of each layer, to ensure a homogeneous thickness growth. The optical thickness and refractive index of each layer were analyzed by "Winspall" software with the transfer matrix evaluation method. Since these two quantities cannot be uniquely determined by this method, one of them must be measured by an independent method. The refractive index of all polyelectrolyte layers was assumed to be 1.54. This assumption was based on a previous work[27] where the refractive index of a PSS/PAH multilayer system was determined by SPR as the thickness was measured by small-angle X-ray reflectivity. Similar values for the refractive index of PSS/PAH multilayers system were found by others.[21,29] Unfortunately, we do not have independent data for the refractive index of the DNA layers. Moreover, as we will discuss later, in certain situations DNA/PAH multilayers are highly porous and therefore might have different (smaller) effective refractive index.[30,31] Therefore, the assumption of a constant refractive index may lead to a certain inaccuracy (underestimation) in the evaluation of optical thicknesses of the DNA layers, as will be discussed below.

2.3.2. AFM Imaging. The morphology and roughness of the multilayer were analyzed by atomic force microscopy (AFM). The sample was assembled on the glass substrate and dried in air. AFM measurements were performed in air using tapping mode (Nanoscope IIIa, Digital Instruments).

(24) Kern, W. *Semicond. Int.* **1984**, 94.

(25) Vinogradova, O. I.; Lebedeva, O. V.; Vasilev, K.; Gong, H.; Garcia-Turiel, J.; Kim, B. S. *Biomacromolecules* **2005**, *6*, 1495−1502.

(26) Decher, G.; Lvov, Y.; Schmitt *Thin Solid Films* **1994**, *244*, 772−777.

(27) Vasilev, K.; Knoll, W.; Kreiter, M. *J. Chem. Phys.* **2004**, *120*, 3439−3445.

(28) Knoll, W. *Annu. Rev. Phys. Chem.* **1998**, *49*, 569−638.

(29) Picart, C.; Sengupta, K.; Schilling, J.; Maurstad, G.; Ladam, G.; Bausch, A. R.; Sackmann, E. *J. Phys. Chem. B* **2004**, *108*, 7196−7205.

(30) Chen, J. T.; Thomas, E. L.; Zimba, C. G.; Rabolt, J. F. *Macromolecules* **1995**, *28*, 5811−5818.

(31) Maldovan, M.; Bockstaller, M. R.; Thomas, E. L.; Carter, W. C. *Appl. Phys. B* **2003**, *76*, 877−884.

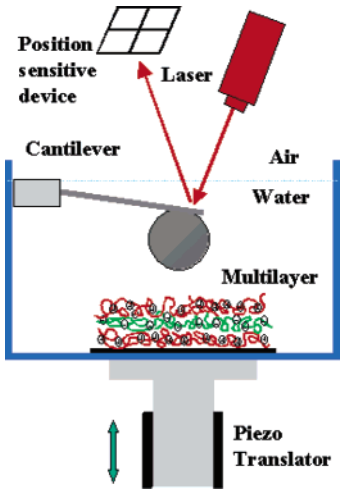

Figure 1. The AFM-related setup used for force measurements.

2.3.3. Force–Distance Measurements. The interaction and adhesion properties of the multilayers were studied with the homemade AFM-related setup (Figure 1) described in detail before.[32−35] Briefly, to measure the force curves the cuvette was moved vertically toward the cantilever with a 12 μm range piezoelectric translator (Physik Instrumente). This translator is equipped with integrated capacitance position sensors, which provide measurements of their actual position and further adjustment of piezo movement. This feature leads to an accuracy of 0.005%, which means that for piezo travel of 12 μm, the maximum error is 0.6 nm. During the movement the deflection of the cantilever was measured with an optical lever technique. For this, the light of a laser diode (3 mW, 670 nm) was focused onto the back of the gold-coated cantilever using microfocusing optics (spot diameter is about 8 μm), and after reflection from the cantilever and from another mirror, the position of the reflected laser spot was measured with a two-dimensional position-sensitive detector (PSD) (SiTek; active area 2×2 cm^2). Glass microspheres were glued onto the apex of the tipless V-shaped cantilevers, using epoxy glue (UHU plus), and the spring constant 0.58 N/m was measured by thermal noise power spectra in a molecular force probe (MFP) 1D (Asylum Co). Glass substrates coated with polyelectrolyte multilayers were placed onto the bottom of a Teflon cuvette. The Teflon cuvette was filled with Milli-Q water. All measurements were done at the driving speed of 200 nm/s to avoid the influence of hydrodynamic drag forces.[34,36]

3. Results and Discussion

3.1. Morphology and Roughness of the Multilayer Films. We started with the study of changes in the surface morphology and roughness during the multilayer buildup. For this purpose, we have taken and analyzed AFM images of multilayers.

The morphology and structure of DNA/PAH films were different, depending on which polyelectrolyte, DNA or PAH, had formed the outer layer. An outer DNA layer always contained large domains of parallel-oriented, elongated "hills" (not shown) similar to what we have observed before for colloidal spheres coated by DNA/PAH films.[25] The formation of this highly ordered lamellar phase in the case of semiflexible polyelectrolytes is consistent with the earlier theoretical predictions.[37] An outer PAH layer of DNA/PAH films always led to a highly porous morphology (Figure 2a). DNA is a rigid polyelectrolyte with a large persistence length ($L_p \sim 50$ nm) in contrast to the highly flexible PAH chains ($L_p \sim 1$ nm). Since DNA is significantly higher in electron density than PAH, it is likely that it is the DNA packing that determines the multilayer structure. This, in particular, leads to a formation of long-range lamellar ordering in the case of an outer DNA layer. The flexible polycations act as simple electrostatically driven linker molecules that can wrap around a single DNA and bridge between DNA strands. This is probably a reason for a highly porous morphology in the case of an outer PAH layer. We remark that a similar scenario is responsible for the structure of bulk DNA/polycation complexes (polyplexes). Indeed, it has been recently reported[38] that polyplexes show hexagonal packing. Like in our experiment, this structure is controlled by the DNA ordering, whereas the internal spacing and the degree of ordering depends on the chemical nature of polycations that act as electrostatic bridges between DNA molecules.

In contrast to DNA/PAH films, a homogeneous coating with low roughness was observed in the case of PSS/PAH multilayers, where both polyelectrolytes are flexible ($L_p \sim 1$ nm). A typical AFM image is shown in Figure 2b. The morphology of PSS/PAH films was found to be independent of the type of outer layer.

The root-mean-square (rms) roughness of DNA/PAH and PSS/PAH multilayers as a function of the number of deposited layers is shown in Figure 3. The change in roughness is much more significant in the case of the DNA/PAH film, especially after assembly of two bilayers. For this film, the rms roughness is larger for an outer DNA layer and smaller for an outer PAH layer. This confirms that PAH adsorbs into the "valley" between "hills" formed by ordered DNA molecules. An interesting observation is that the roughness increases with the number of bilayers. In contrast, roughness changes observed for PSS/PAH films with the layer numbers are small. The rms value is on the same order as that for bare glass surfaces. Also, no dependence of rms value on the polyelectrolyte charge and/or layer number was observed for PSS/PAH films under our assembly conditions.

3.2. Multilayer Film Thickness. An equilibrium optical film thickness of PSS/PAH and DNA/PAH multilayers was studied as a function of the number of deposited layers. Both films were assembled on a PEI prelayer (Figure 2). The thickness of the first deposited bilayer was found to be the same for PSS/PAH and DNA/PAH films.

The clear linear growth of the assembly in the case of a PSS/PAH system suggests similar adsorption properties for both polyelectrolytes. The thickness of a PSS monolayer is found to be approximately 2 nm and of a PAH monolayer about 1.5 nm. These results are in agreement with previous studies performed with different techniques.[15,21]

On the contrary, a much larger increase in the film thickness was observed for the DNA/PAH film starting from the second bilayer. The DNA/PAH multilayer shows a nonlinear thickness growth of the assembly (Figure 4) although it can be regarded as linear after the fifth layer. It has been previously suggested that the high molecular weight semiflexible DNA molecules can form surface (vertical) loops during the adsorption.[25,37] Our results here

(32) Yakubov, G. E.; Butt, H. J.; Vinogradova, O. I. *J. Phys. Chem. B* **2000**, *104*, 3407−3410.
(33) Vinogradova, O. I.; Yakubov, G. E.; Butt, H. J. *J. Chem. Phys.* **2001**, *114*, 8124−8131.
(34) Vinogradova, O. I.; Yakubov, G. E. *Langmuir* **2003**, *19*, 1227−1234.
(35) Ecke, S.; Raiteri, R.; Bonaccurso, E.; Reiner, C.; Deiseroth, H. J.; Butt, H. J. *Rev. Sci. Instrum.* **2001**, *72*, 4164−4170.
(36) Vinogradova, O. I.; Butt, H. J.; Yakubov, G. E.; Feuillebois, F. *Rev. Sci. Instrum.* **2001**, *72*, 2330−2339.
(37) Netz, R. R.; Joanny, J. F. *Macromolecules* **1999**, *32*, 9013−9025.
(38) DeRouchey, J.; Netz, R. R.; Rädler, J. O. *Eur. Phys. J. E* **2005**, *16*, 17−28.

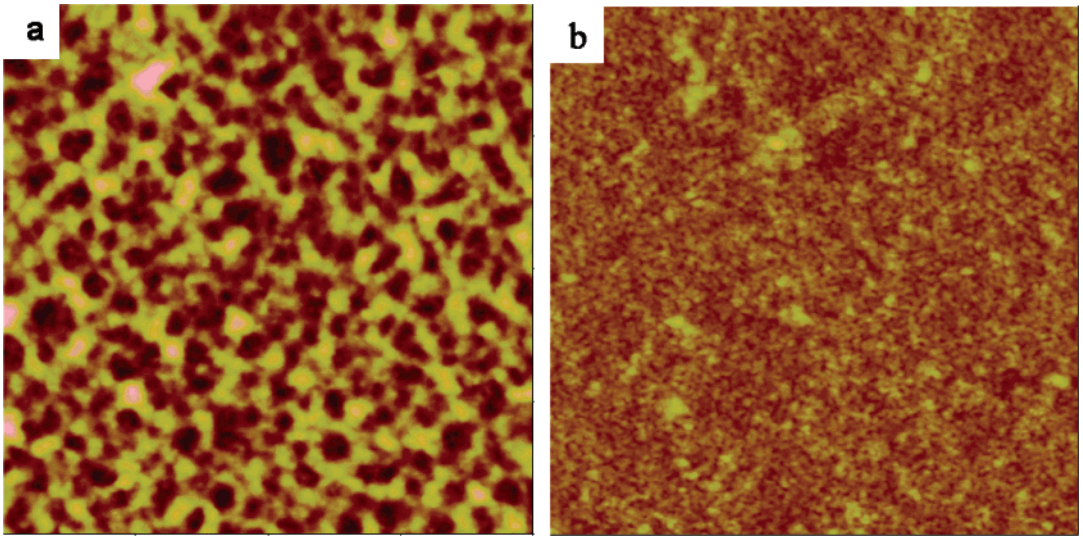

Figure 2. AFM height images PEI−DNA−PAH (a) and PEI−PSS−PAH (b) multilayers. The sample was assembled without drying and measured in air. The scan area is 1 μm × 1 μm.

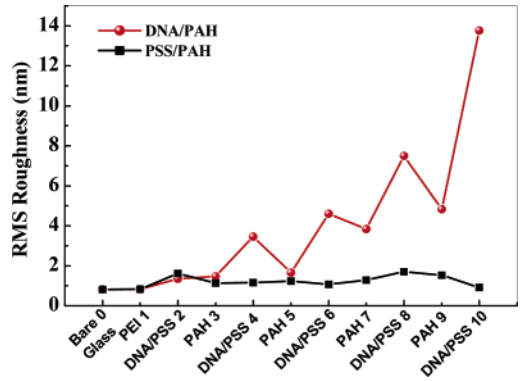

Figure 3. Root-mean-square roughness of PSS/PAH film and DNA/PAH multilayer estimated from AFM height images.

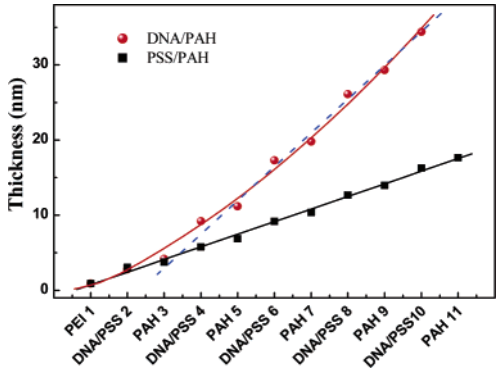

Figure 4. Equilibrium optical thickness of the growing PSS/PAH and DNA/PAH multiyears measured by surface plasmon resonance spectroscopy. The concentration of the aqueous polyelectrolyte solutions was 1 mg/mL for all, except for DNA (0.5 mg/mL), with a NaCl concentration of 0.5 M. The solid line represents the best polynomial fits.

obtained with a PEI prelayer are in agreement with this concept. The DNA monolayer thickness (5−6 nm) is much larger than the PAH monolayer thickness (1−3 nm). This is in agreement with the AFM data and confirms that PAH molecules due to their flexibility adsorb mostly into valleys of the DNA loops, acting as bridges between DNA strands. An increased thickness for the DNA layer is observed, with the layer number almost likely to indicate that DNA may take a different configuration with the growing of the multilayer. While the first DNA layer may form horizontal loops (i.e. lie flat on the surface), the next DNA layers form vertical loops. These results disagree with measurements made before,[39] where the DNA monolayer thickness was found to be smaller than we observe here. This is likely due to use of adsorption solutions with different concentrations of DNA and NaCl. Another reason could be that in ref 39 the thickness of dried film was studied, but here we are measuring the multilayers immersed in water.

We note that the porosity of DNA/PAH multilayers may lead to its smaller density, and, therefore, a smaller refractive index as compared with what we have assumed. As a result, the optical thickness we found for this multilayer might be slightly underestimated. The estimates made with the physically realistic smaller values of refractive index[30] (1.48) suggest that the thickness of a single DNA layer can be as large as 6.5 nm. In other words, the mistake we might introduce by assuming that the DNA/PAH film is uniform can be up to ~20%. This, however, cannot change our conclusions, since it gives even larger differences from PSS/PAH multilayers than reported above. The same remark concerns the possible influence of the roughness of the DNA/PAH film on the results of optical measurements. However, we remind the reader that the SPR measurements were performed in water, while the rms data correspond to dried films. Clearly, the multilayers in water should be smoother than after drying. Therefore, we do not expect that the roughness of DNA/PAH films had some significant implications on our SPR results.

3.3. Force−Distance Profiles. To study the interaction and adhesion properties of multilayers, force−distance curves were measured after a deposition of each monolayer. Multilayers were assembled both with and without drying. Figure 5 shows two typical force−distance curves for $(PSS/PAH)_2$−PSS and $(PSS/PAH)_3$ multilayers assembled with drying. It can be seen that, when an outer layer is formed by polyanions, the forces are repulsive. There is no hysteresis between forces measured on approach and retract, and no pull-off force was detected in the case of an outer layer formed by polyanions. This confirms that the multilayer is negatively charged due to the overcompensation of the surface charge during as-

(39) Lvov, Y.; Decher, G.; Sukhorukov, G. B. *Macromolecules* **1993**, *26*, 5396−5399.

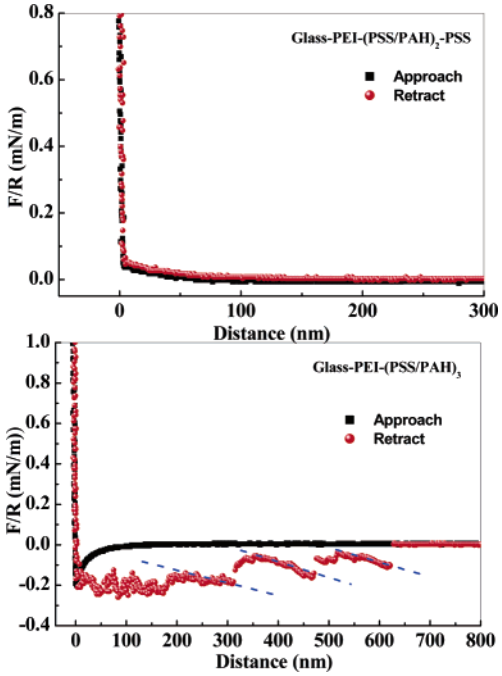

Figure 5. Force−distance curves for the multilayer of PEI−$(PSS/PAH)_2$−PSS and PEI−$(PSS/PAH)_3$ assembled with drying. The dashed lines indicate the multiple adhesions.

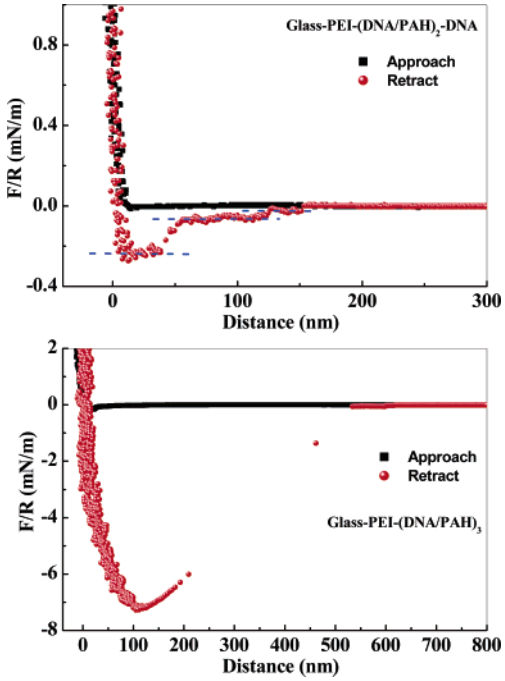

Figure 6. Force−distance curves for the multilayer of PEI−$(DNA/PAH)_2$−DNA and PEI−$(DNA/PAH)_3$ assembled with drying. The dashed lines indicate the plateau regions in the retract curves.

sembly.[40] When an outer layer is formed by polycations, the approach curves show a long-range attraction (up to 100 nm). This is likely caused by strong electrostatic attractive forces between a negatively charged glass particle and a positively charged multilayer. In the retract curve, strong adhesion with a sawtooth pattern is observed (dashed lines in Figure 5). The range of adhesion forces is above 600 nm, which is much larger than the contour length of PAH (187 nm) and PSS (91 nm).[41] Therefore, the multiple adhesion can be attributed to a bridge, formed by entangled PAH and PSS chains, between the particle and the multilayer, as shown in Figure 7. The unfolding of each polymer chain leads to the sawtooth pattern of the retract curve. Note, that a similar effect was observed during the extension of fused phospholipids bilayers[42] and was also attributed to a multiple bridging. An important point to note is that the multiple adhesion is only observed in the case of an outer PAH layer, which indicates that the adsorption of the positive charged PAH chain on the negative glass particle is essential for this kind of multiple chain bridge. All other curves measured with different numbers of layers in the film have the same characters, although the values of pull-off forces vary.

Figure 6 shows the typical force−distance curves obtained for DNA/PAH multilayers assembled with drying. If an outer layer was formed by DNA, the force−distance curves always show electrostatic repulsion force on approach, reflecting the negative surface charge of the multilayer. Moreover, the concave contact curve suggests that the film is soft and the DNA loops on the surface are compressible. This observation is different from what we had for PSS/PAH multilayers, where the quasirigid contact lines were found. In the retract curve, a weak attractive force is observed with some plateau regions, as indicated by the dashed lines. If an outer layer was formed by PAH, we have observed attractive forces on approach. However, they were of much shorter range than in the case of PSS/PAH multilayers. One can speculate that this is connected with the lower surface charge density. The retract curves always show a large single adhesion peak. The range of the pull-off force is ~600 nm. This value exceeds the contour length of PAH but is well below the contour length of DNA (~3 μm). This is likely due to entanglement of PAH/DNA chains causing partial detachment of adsorbed DNA layers (Figure 7).

The same measurements were performed with the multilayers assembled without drying, and similar trends were observed. As a rule, the picture was qualitatively the same except as for the first PSS layer, where we sometimes have seen an attractive force on approach. This is probably connected with the heterogeneity in the surface charge.

3.4. Adhesion Force Change of the Multilayer Buildups. As described above, the force−distance curves are different for films with positively and negatively charged outer layers. Figure 8 shows the maximum pull-off force measured for PSS/PAH multilayers as a function of the number of deposited layers. Data include the results of measurements performed with the multilayers assembled both with and without drying. The (maximum) pull-off force is defined as the minimum of the retract curve. Every point represents an average of several (minimum of four) values of the pull-off force. The error bars show the standard deviation (scatter of the data). It is seen that there are both similarities and differences between multilayers deposited with and without drying. In case of multilayers assembled with drying, regular oscillations in the pull-off forces with increasing layer number are observed. No pull-off forces are observed when PSS was an outer layer. A discernible adhesion is found when PAH served as an outer layer.

For the multilayers assembled without drying, some differences are observed for the first several monolayers. One can conclude that the assembly with drying allows one to create a more regular multilayer structure.

(40) Ladam, G.; Schaad, P.; Voegel, J. C.; Schaaf, P.; Decher, G.; Cuisinier, F. *Langmuir* **2000**, *16*, 1249.
(41) Adamcyk, Z.; Zembala, M.; Warszynski, P.; Jachimska, B. **2004**, *20*, 10517.
(42) Maeda, N.; Senden, T. J.; di Meglio, J. M. *Biochim. Biophys. Acta* **2002**, *1564*, 165−172.

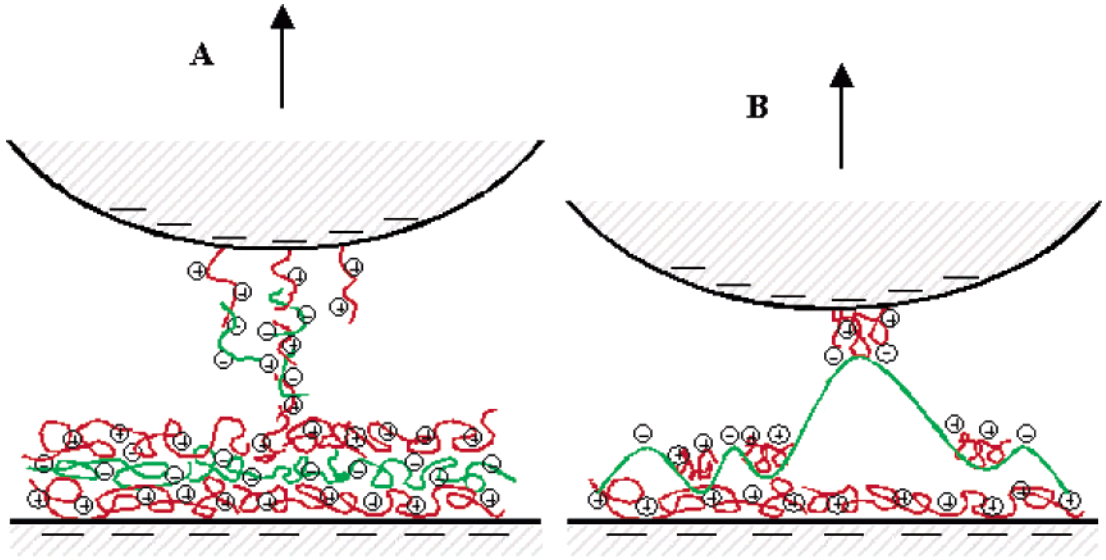

Figure 7. Schematic illustration of the interactions between glass particle and PSS/PAH multilayer (A) and DNA/PAH multilayer (B).

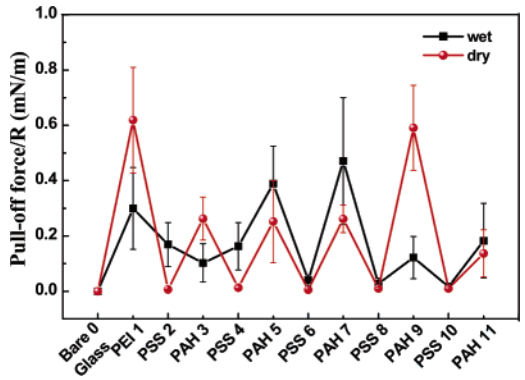

Figure 8. Pull-off forces change as a function of layer number for PSS/PAH multilayers assembled with and without drying. The error bars represent the scatter of the data obtained from different areas in the sample.

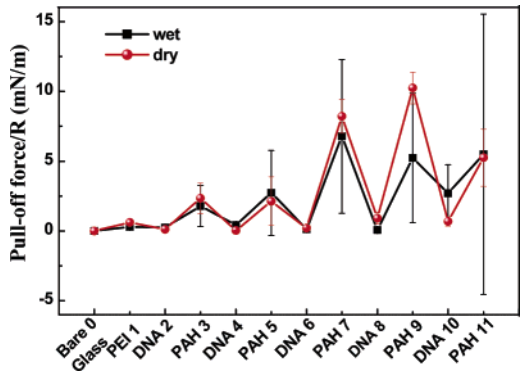

Figure 9. Pull-off force changes as a function of layer number for DNA/PAH multilayers assembled with and without drying. The error bars represent the scatter of the data obtained from different areas in the sample.

Figure 9 shows the pull-off forces measured for DNA/PAH multilayers as a function of the number of layers, again assembled with and without drying. As compared with the PSS/PAH films, much stronger adhesive forces are observed in case of positively charged DNA/PAH multilayers. For these films, we also observe the regular oscillation of maximum pull-off forces. Moreover, in case of positively charged films, the pull-off forces increase with the layer number. We note, that the scatter in pull-off force data is much larger in the case of PAH as an outer layer, especially in the case of assembly without drying.

4. Conclusion

In this paper we have studied the growth, structure, and morphology, as well as interaction and adhesion properties of PSS/PAH and DNA/PAH multilayers. Multilayers assembled both with and without drying have been investigated. We have shown that PSS/PAH multilayers, based on highly flexible polyelectrolytes, have uniform and smooth surface morphology and grow linearly. In contrast, DNA/PAH multilayers, containing both flexible and semiflexible polyelectrolytes, show rough morphology and highly heterogeneous structure. Depending on the type of polyelectrolyte that formed an outer layer, we have observed a long-range lamellar ordering (DNA) or a porous structure (PAH). The lamellar phase indicates the DNA packing, while the porous structure suggests that flexible polycations act as linkers that wrap around a single DNA as well as bridge between DNA strands. Additionally, DNA/PAH multilayers were found to grow nonlinearly. The difference in multilayer structure and morphology led to a difference in interaction and especially adhesion properties. The negatively charged PSS/PAH multilayers have shown no adhesion to the surface of a negatively charged glass sphere, while the negatively charged DNA/PAH multilayers revealed a small, but discernible, pull-off force with several plateau regions. The pull-off force of positively charged PSS/PAH multilayers shows a long-range sawtooth profile, while a single adhesion peak of similar range but with a much larger amplitude was observed in case of a positively charged DNA/PAH film. We have interpreted these results in terms of multiple bridging of polyelectrolyte chains and related them to a structure and a morphology of the multilayers.

Acknowledgment. H.G. acknowledges the support of the Alexander von Humboldt Foundation, and J.G.T. acknowledges the support within the Marie Curie Training Site program. This work was partly supported by a DFG priority program "Micro and Nanofluidics" (Vi 243/1-1) and by the RAS program "Macromolecules and Micromolecular Structures of New Generations". We have benefited from valuable discussions with B.S. Kim, W. Knoll, K. Koynov, O.V. Lebedeva, and H. Schiessel.

LA051045M